

MEDSI 2008

Mechanical Engineering Design for Synchrotron Radiation
Instrumentation in Saskatoon, Saskatchewan, Canada. June 2008

Development of the Crotch Absorbers for ALBA Storage Ring

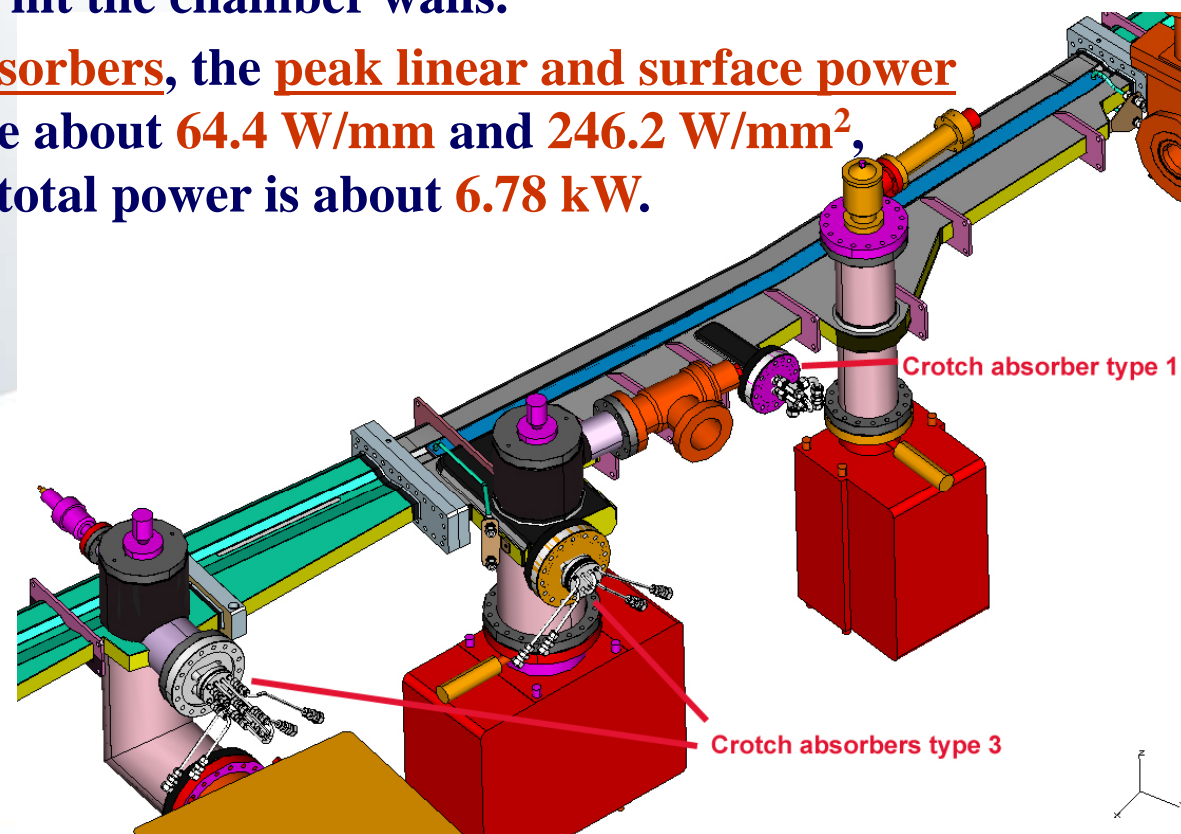
Marcos Quispe

In collaboration with E. Al-Dmour, D. Einfeld, R. Martin, L.
Nikitina, and L. Ribó

- 1. Introduction.**
- 2. Conservative approach for the Bending Magnet (BM) radiation.**
- 3. The design criteria.**
- 4. Basic design.**
- 5. Cooling boundary conditions.**
- 6. Finite Element Analysis (FEA).**
- 7. Optimization of the model.**
 - Optimization of the tooth
 - Optimization of the end of the pinholes.
- 8. Hydraulic tests for real models.**
- 9. Conclusions.**

1. The ALBA Synchrotron Light Facility is a third generation light source with a storage ring of 268.8 m in circumference.
2. Its beam energy and design current are 3 GeV and 400 mA respectively.
3. With the design current, a total power of 407 kW is radiated by the circulating beam from the 32 bending magnets.
4. The ALBA crotch absorbers follow the original design done at ANKA.
5. In total 156 crotch absorbers are needed all around the machine in order to guarantee that no radiation will hit the chamber walls.
6. For the ALBA critical crotch absorbers, the peak linear and surface power densities at normal incidence are about 64.4 W/mm and 246.2 W/mm², respectively, and the maximum total power is about 6.78 kW.

Figure 1 Several absorber after each dipole to guarantee no radiation will hit the vacuum chamber



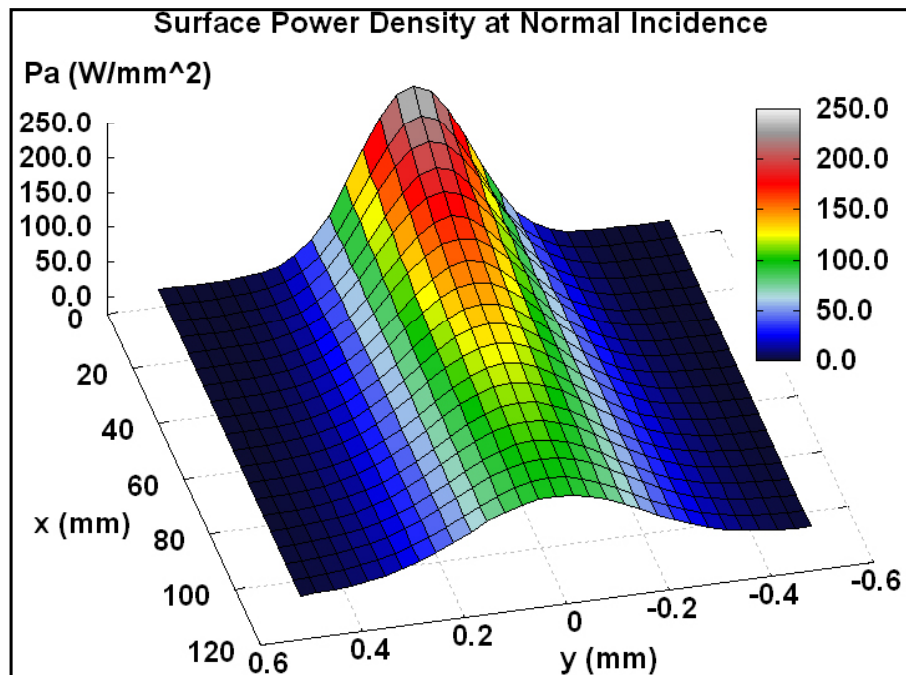
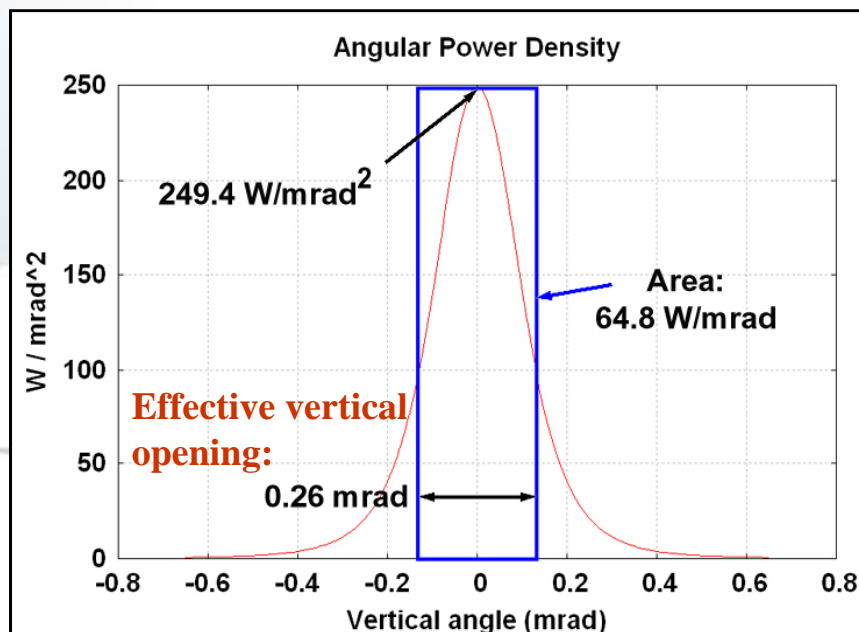


Figure 2 (top): Example of how the **footprint heating** on the critical crotch absorbers surface spreads out in an extensively wider area along the x–horizontal direction than along the y–vertical direction.

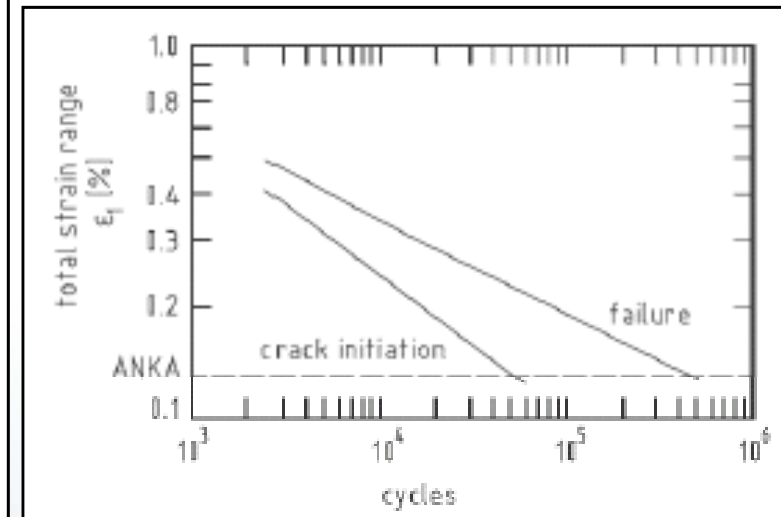
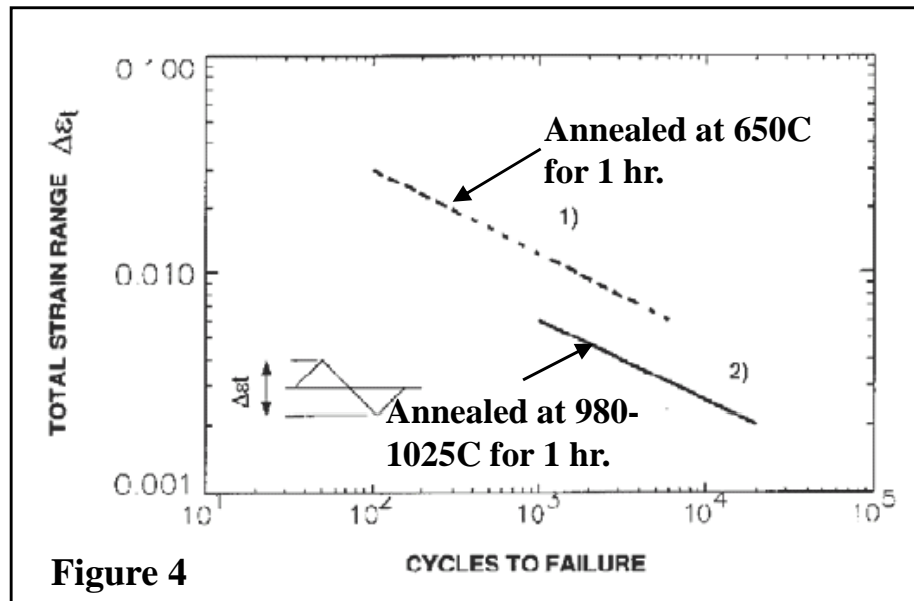
Figure 3 (right): **Conservative approach** for the thermal boundary condition. The area below the angular power density is included in a rectangular area.

Table 1: Main parameters for ALBA Storage Ring which characterize the power on the absorbers.

Parameter	Unit	Values
Beam Energy, E	GeV	3
Design current, I	mA	400
Dipole magnetic field, B	T	1.42
Dipole magnets radius of curvature, ρ	m	7.047



ANKA / SLS. A strain value for **OFHC** copper of less than **0.2%** which guarantee a **10,000 cycle** was considered reasonable design criteria (S. Hermle et al, PAC 1999).



ESRF. (L. Zhang et al, MEDSI 2002)

Proposed design criteria for copper absorbers (BM rad. power):

$$\sigma_{\max}^{\text{VM}} < 2 * S_{\text{ultimate}} \quad 400 \text{ MPa for OFHC copper}$$

$$\sigma_{\max}^{\text{VM}} < 2 * S_{\text{ultimate}} \quad 850 \text{ MPa for GlidCop}$$

$\sigma_{\max}^{\text{VM}}$: *calculated maximum Von Mises stress with the elastic assumption*

APS. (M. Choi et al, PAC 1999).

Thermal Condition

$$T_{\text{water}} < T_{\text{boil}} = 150^{\circ}\text{C at 5 ATM}$$

$$T_{\text{surf}} < 0.5 \times T_{\text{melt}} = 541^{\circ}\text{C for Copper}$$

Structural Condition

$$\begin{aligned} &\text{Thermal Stress} < 2 \times S_Y(0.2\% \text{ Yield Strength}) \\ &\text{and} \\ &< S_f(\text{Fatigue Strength}) \text{ for } 10^5 \text{ Cycles} \\ &\text{and} \\ &\text{Thermal Stress} < S_2(\text{Hot}) + S_2(\text{Cold}) \end{aligned}$$

$$\Delta T_{\text{max}} < 300^{\circ}\text{C for Glidcop}$$

$$\Delta T_{\text{max}} < 150^{\circ}\text{C for OFHC copper}$$

DIAMOND. (Hou-Cheng Huang, DIAMOND 2004)

0.5% peak strain (50 MPa) and 0.1% (35 MPa) in the bulk body of the copper absorber

Copper:

The low cycle fatigue behaviour of OFHC copper at 300°C in high vacuum. For brazed (30 min at 980°C followed by 2 min hold at 1,025°C) and unbrazed specimen and for two sizes of specimen (K.C. Liu et al, JNM, 1984).

Glidcop Al-15

The cycles for fatigue for Glidcop Al-15 at 100, 200, 400 and 600°C for heat treated (800°C for 3 hours) for Glidcop specimen . (Sunao Takahashi at al, MEDSI 2006).

The material has been chosen for cycles more than 1×10^5 cycles of OFHC copper (strain = 0.1%) and over 1×10^5 cycles for Glidcop Al-15 (strain = 0.2%).

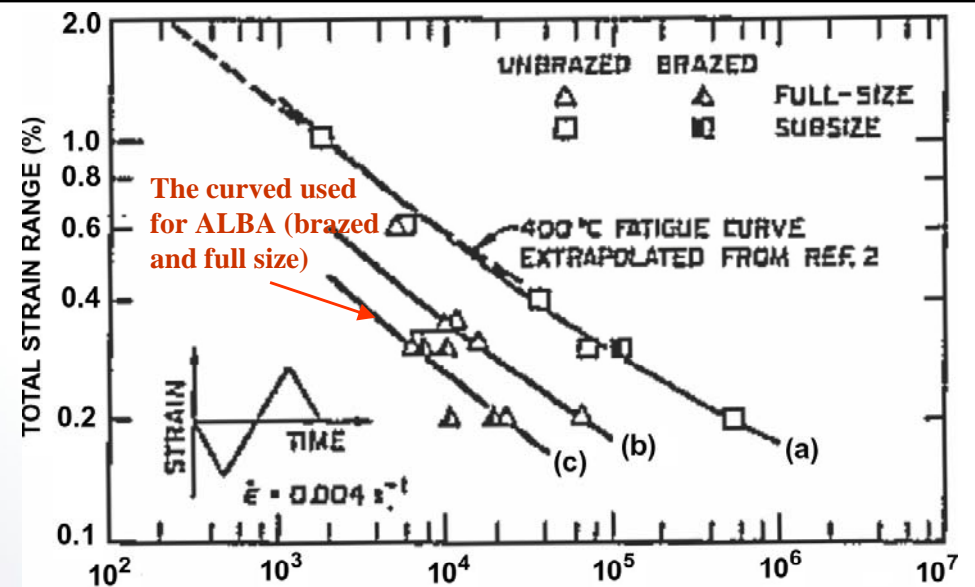


Figure 6 CYCLES TO FAILURE

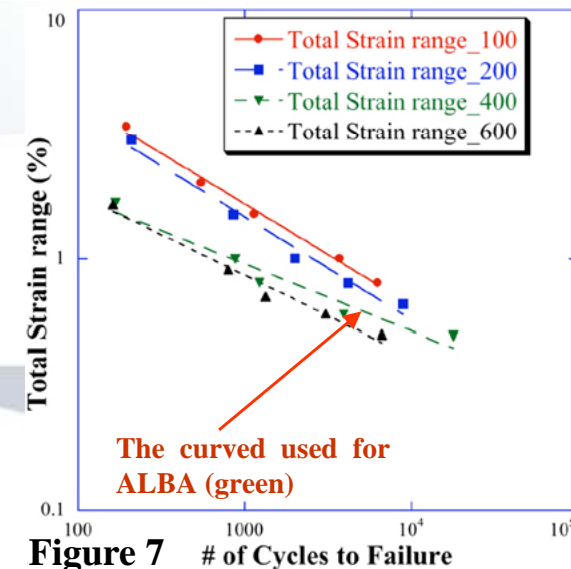


Figure 7 # of Cycles to Failure

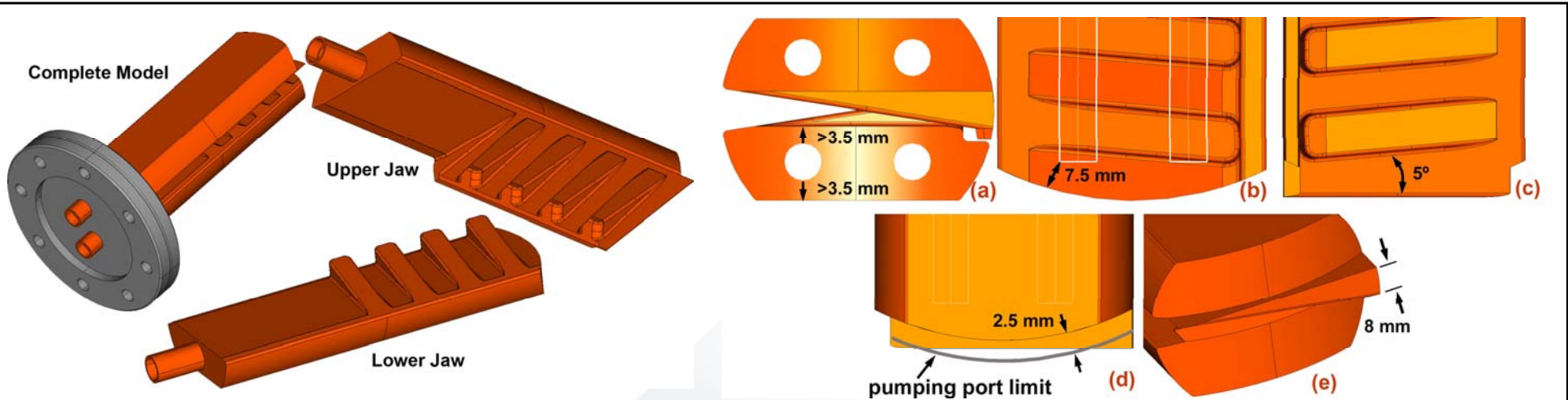


Figure 8 Basic components of the crotch absorber based on the ANKA design.

Figure 9 Some geometrical guidelines for the dimensioning of the ALBA crotch absorbers.

Figure 10 The three types of the crotch absorbers for ALBA (upper jaws). The types 1 and 2 are made of OFHC copper and type 3 is made of Glidcop Al-15.

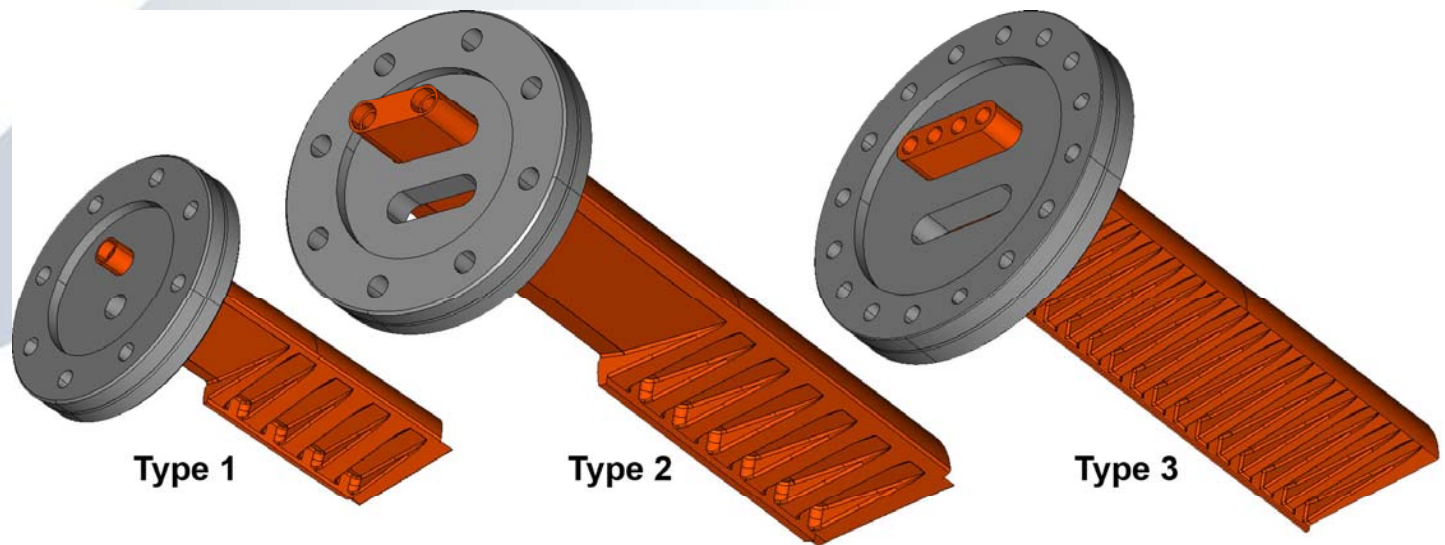


Figure 11 Inner tubes to be inserted into the pinholes (models for ALBA crotch absorber type 1).

ALBA criteria: the velocity in the cooling channels is kept in the range not more than 3 m/s.

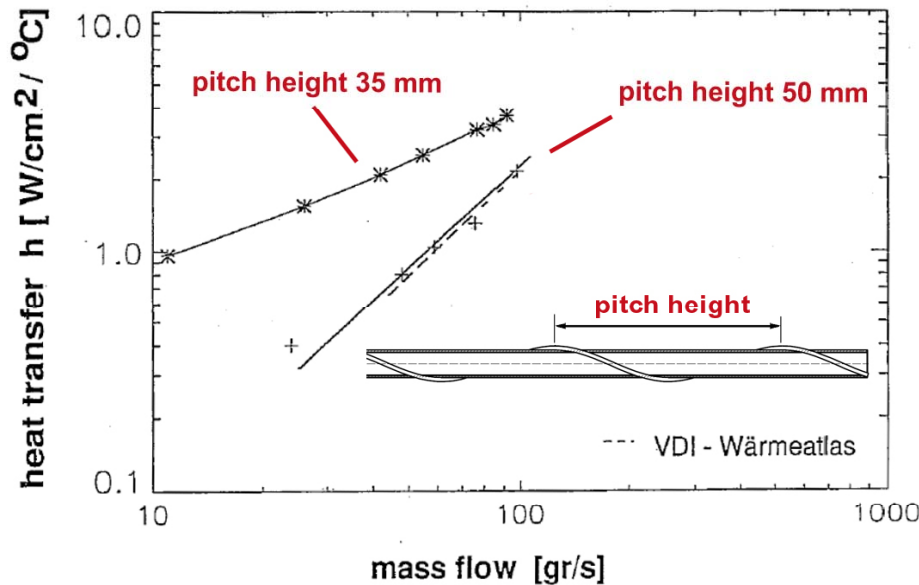


Figure 12 Dependence of the convective heat transfer coefficient “ h ” on the mass flow for two pitch height: 35 and 50 mm (SLS reference).

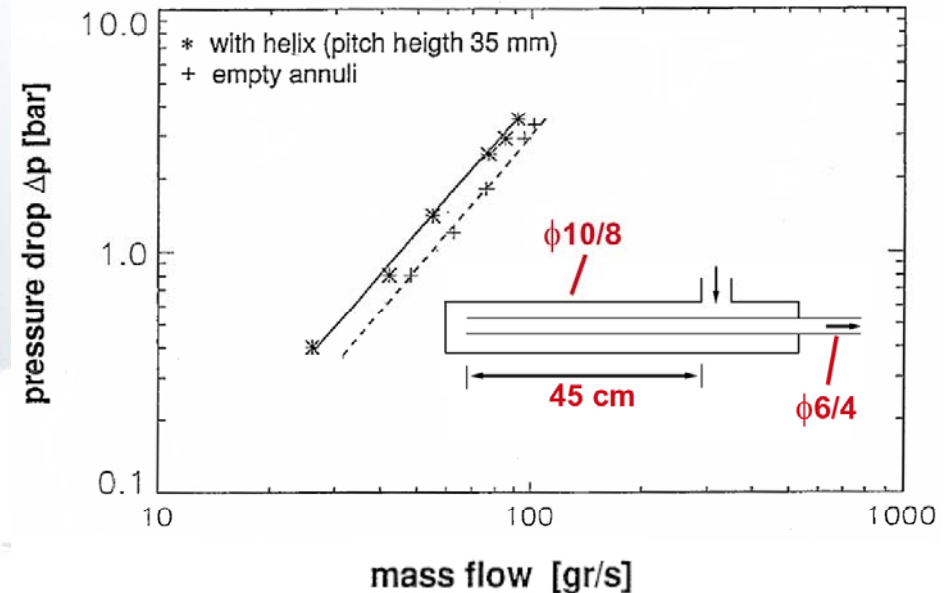


Figure 13 Dependence of the pressure drop on the mass flow for two cases: (i) with helix (pitch height 35 mm) and (ii) empty annuli (SLS reference).

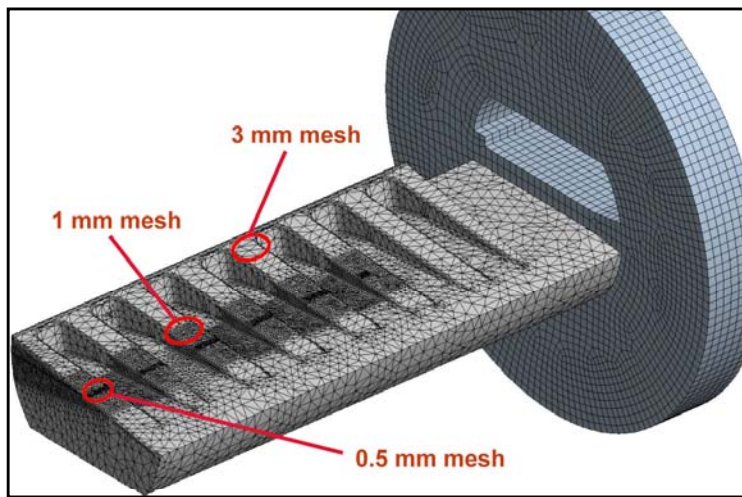


Figure 14 Example of the mesh size used for the simulations. For the numerical optimization the mesh is refined at the footprint.

- The **thermal–stress** analysis was investigated using the **FEA ANSYS** software, based on linear elastic analysis.
- For the power load conditions **three trajectories** of the beam has been investigated:
 - (i) Nominal,
 - (ii) Lower misalignment, and
 - (iii) Upper misalignment
- Materials:
 - (i) **OFHC copper**: **constant** physical properties ($T_{MAX} < 130^{\circ}C$)
 - (ii) **Glidcop Al–15**: physical properties as a **function of the temperature** ($T_{MAX} > 200^{\circ}C$)
- **Variable meshing** concentrate at the footprint.
- The simulation is made only for the **upper jaw**, which is the most **critical part** from the power load point of view.
- The absorbers are cooling by **water** at $23^{\circ}C$.
- **Thermal conditions**: power densities, water cooling at interfaces and adiabatic boundaries.
- **Structural conditions**: temperature map and artificial mechanical constrains to obtain **pure thermal stress**.

6. Finite Element Analysis (FEA): The three types

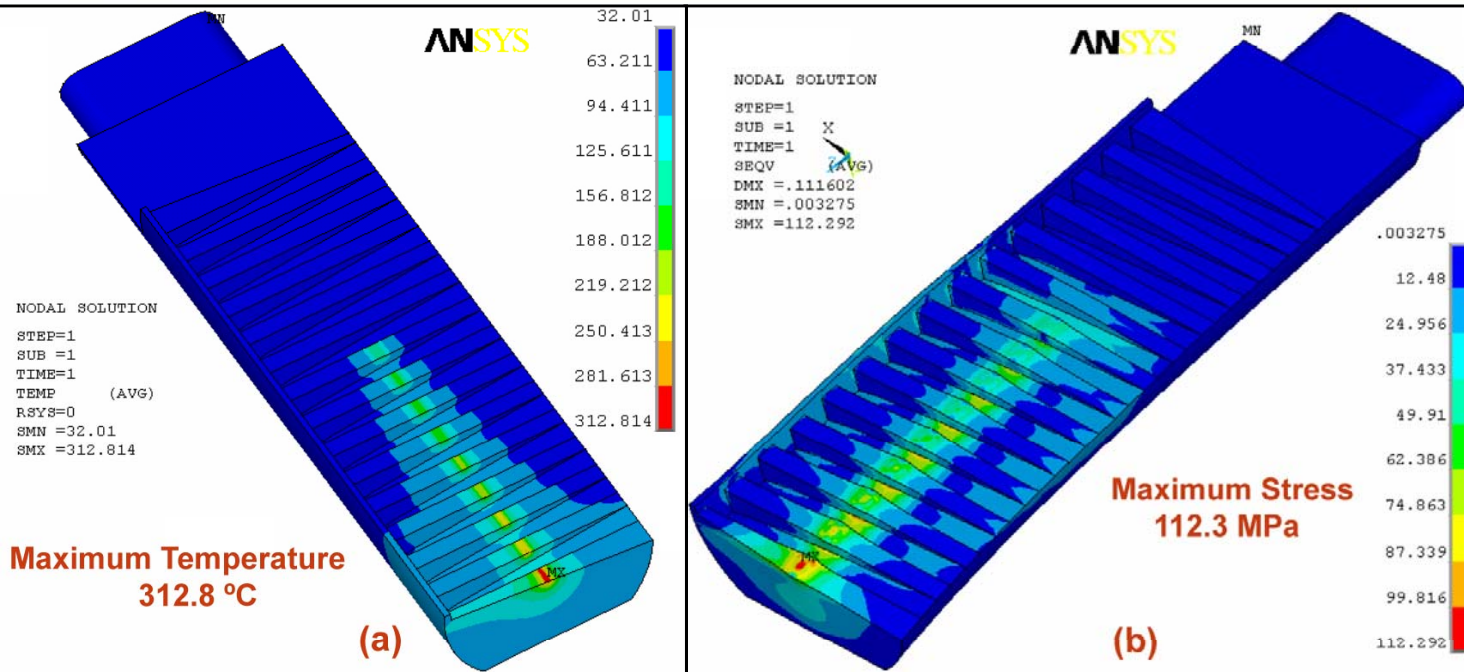


Figure 15 FEA results for absorber **type 3** under conservative **assumption 1**. (a) Temperature distribution. (b) Von Misses stress distribution. (c) Strain distribution. (d) Temperature distribution at cooling wall.



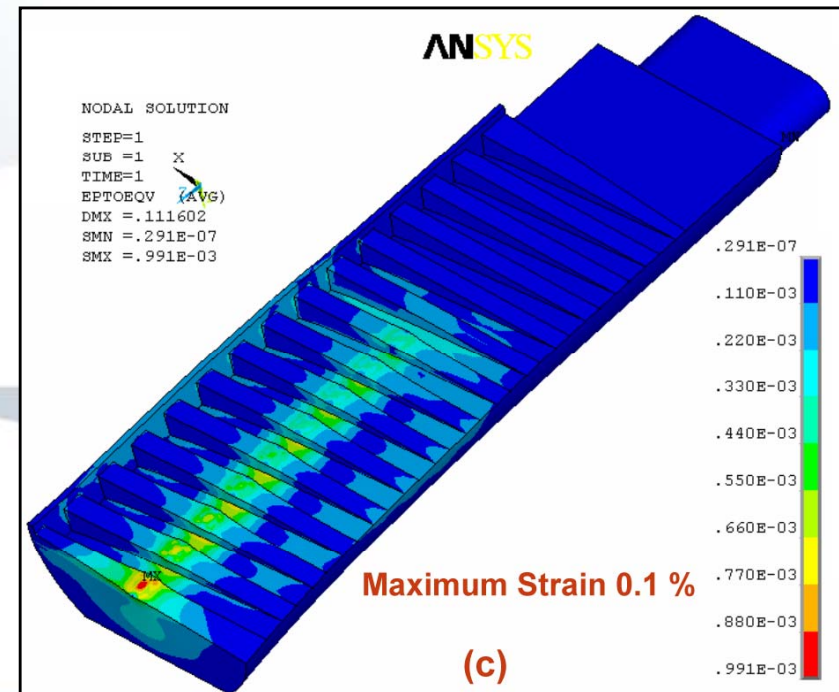
Table 2: FEA results for the three types of the absorbers

Assumption 1 ($h=10,000 \text{ W/m}^2\text{°C}$)				
Absorber Type	$T_{ov, \text{max}} \text{ (°C)}$	$T_c, \text{max} \text{ (°C)}$	Stress (MPa)	Strain (%)
1	91.2	62	21.8	0.019
2	127.5	66	45.8	0.044
3	312.8	91.3	112.3	0.10

significant drop

little variation

Assumption 2 ($h=15,000 \text{ W/m}^2\text{°C}$)				
Absorber Type	$T_{ov, \text{max}} \text{ (°C)}$	$T_c, \text{max} \text{ (°C)}$	Stress (MPa)	Strain (%)
1	79	51	20	0.018
2	109	50	46.3	0.04
3	290	70	111.9	0.098



6. Finite Element Analysis (FEA): Lower misalignment

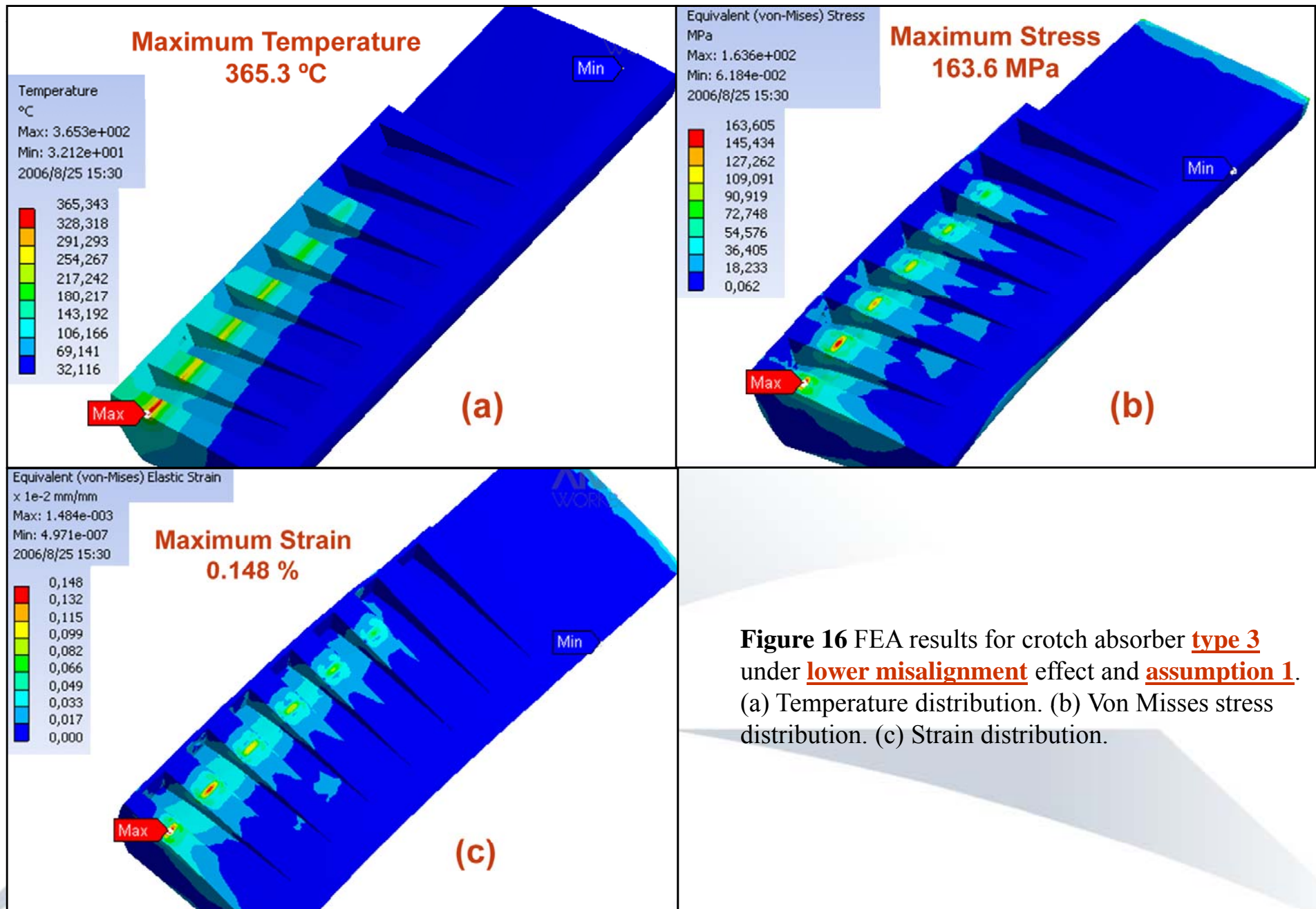


Figure 16 FEA results for crotch absorber type 3 under lower misalignment effect and assumption 1. (a) Temperature distribution. (b) Von Misses stress distribution. (c) Strain distribution.

6. Finite Element Analysis (FEA): Upper misalignment

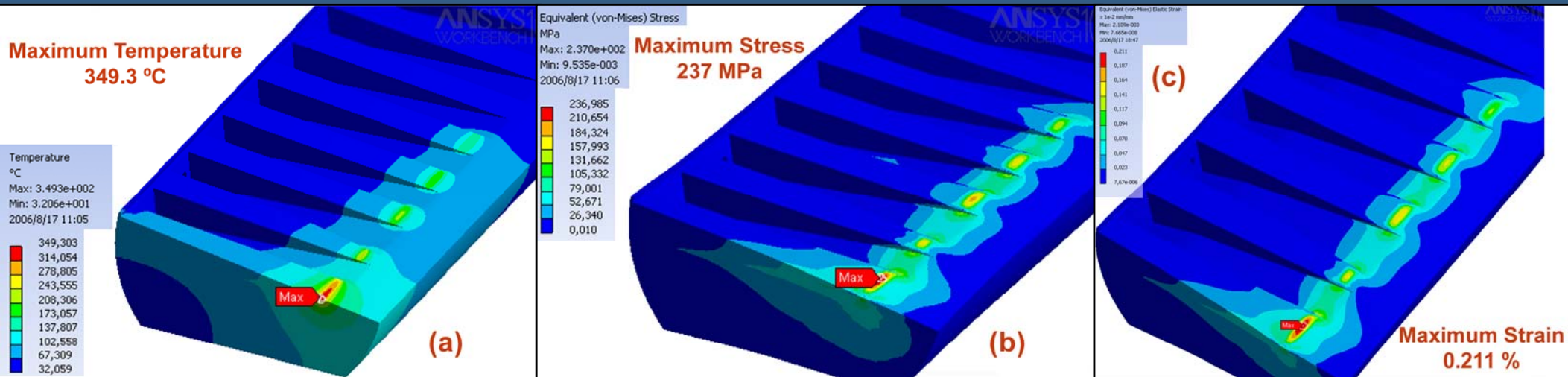


Figure 17 FEA results for crotch absorber **type 3** under **upper misalignment** effect and **assumption 1**. (a) Temperature distribution. (b) Von Misses stress distribution. (c) Strain distribution.

Table 3: FEA results for the crotch absorber type 3 (tooth thickness = 10 mm, tooth inclination = 8.8°) under nominal and misalignment conditions for assumptions 1 and 2.

<i>Assumption 1 ($h= 10,000 \text{ W/m}^2\text{°C}$)</i>				
<i>BM radiation trajectory</i>	<i>T_{ov}, max (°C)</i>	<i>T_c, max (°C)</i>	<i>Stress (MPa)</i>	<i>Strain (%)</i>
<i>Nominal</i>	308	95	195	0.173
<i>Upper Misalignment</i>	349.3 ↑	137.5 ↑	237 ↑	0.211 ↑
<i>Lower Misalignment</i>	365.3 ↑	114 ↑	163.6 ↓	0.148 ↓

Increment in temperature

High increment

Significant drop

<i>Assumption 2 ($h= 15,000 \text{ W/m}^2\text{°C}$)</i>				
<i>BM radiation trajectory</i>	<i>T_{ov}, max (°C)</i>	<i>T_c, max (°C)</i>	<i>Stress (MPa)</i>	<i>Strain (%)</i>
<i>Nominal</i>	285	73	193	0.169
<i>Upper Misalignment</i>	322	110	234	0.206
<i>Lower Misalignment</i>	340	89	162	0.145

7. Finite Element Analysis (FEA): Tooth design optimization

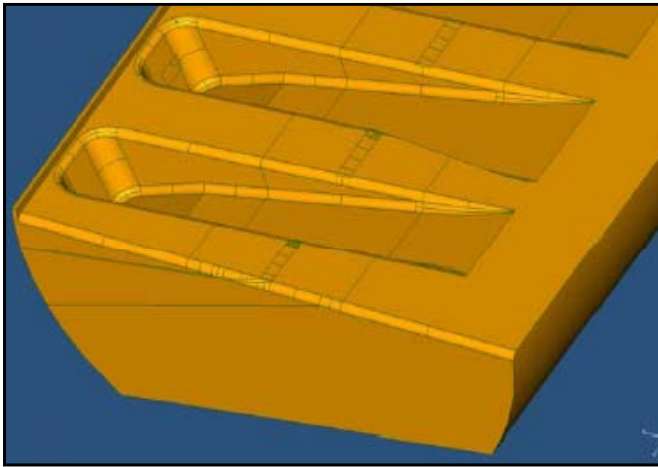


Fig. 18 Model 1:
tooth thickness = 10 mm
tooth inclination = 8.8°

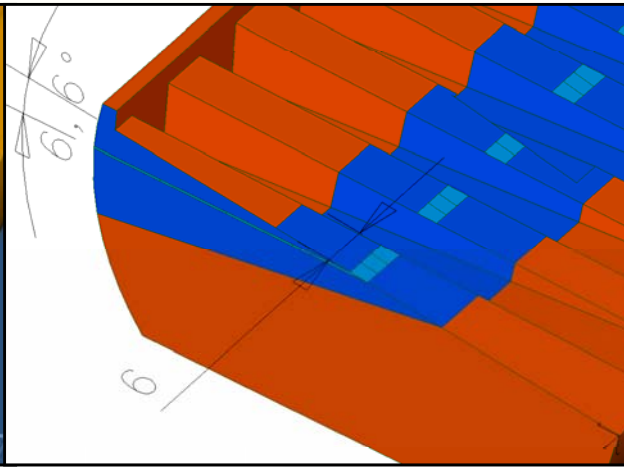


Fig. 19 Model 2:
tooth thickness = 6 mm
tooth inclination = 6.6°

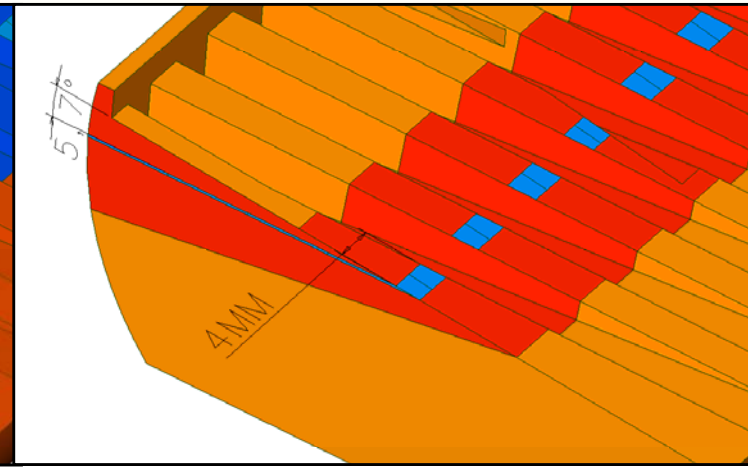


Fig. 20 Model 3:
tooth thickness = 4 mm
tooth inclination = 5.7°

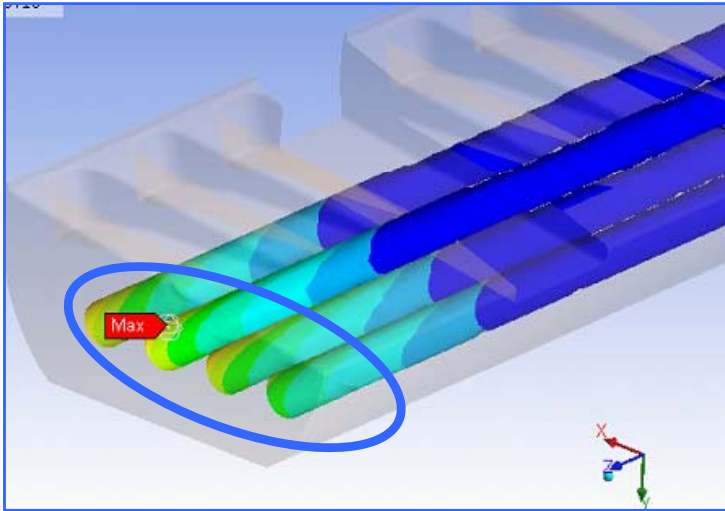
Table 4: Comparative studies for the three models of the crotch absorber type 3. The geometrical differences are the thickness (δ) and the inclination (α) of the tooth.

<i>Assumption 1 ($h= 10,000 W/m^2\text{°C}$)</i>				
<i>Models</i>	<i>Tov, max (°C)</i>	<i>Tc, max (°C)</i>	<i>Stress (MPa)</i>	<i>Strain (%)</i>
1) $\delta = 10 \text{ mm}, \alpha = 8.8^\circ$	308	95	195	0.173
2) $\delta = 6 \text{ mm}, \alpha = 6.6^\circ$	301	92.5	107	0.094
3) $\delta = 4 \text{ mm}, \alpha = 5.7^\circ$	289	89	96	0.081

The temperatures decrease in modest manner

The variable decrease considerably

<i>Assumption 2 ($h= 15,000 W/m^2\text{°C}$)</i>				
<i>Models</i>	<i>Tov, max (°C)</i>	<i>Tc, max (°C)</i>	<i>Stress (MPa)</i>	<i>Strain (%)</i>
1) $\delta = 10 \text{ mm}, \alpha = 8.8^\circ$	285	73	193	0.169
2) $\delta = 6 \text{ mm}, \alpha = 6.6^\circ$	282	71	106	0.092
3) $\delta = 4 \text{ mm}, \alpha = 5.7^\circ$	267	68	96	0.08



The **peak** for temperature, stress and strain are located close to the end of the pinhole, and in there is found the **maximum cooling wall temperature**.

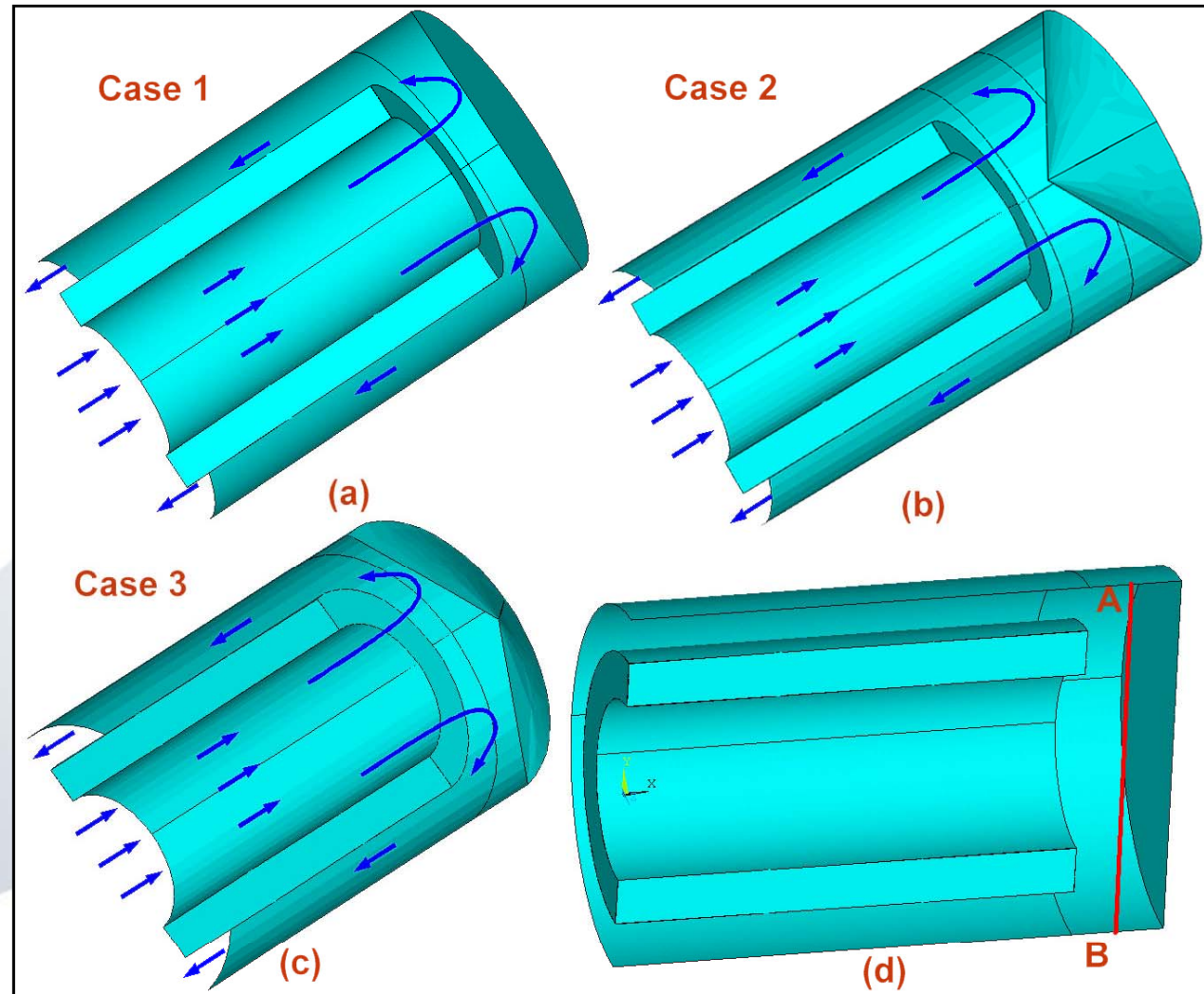


Figure 21 Cases to be analyzed with Computational Fluid Dynamics: (a) Case 1: flat, (b) Case 2: concave inside and (c) Case 3: concave outside. (d) For the comparative study the velocity profiles are analyzed in various positions at the end of the pinhole, like the line represented by AB.

7. Computational Fluid Dynamics (CFD): Pinhole optimization

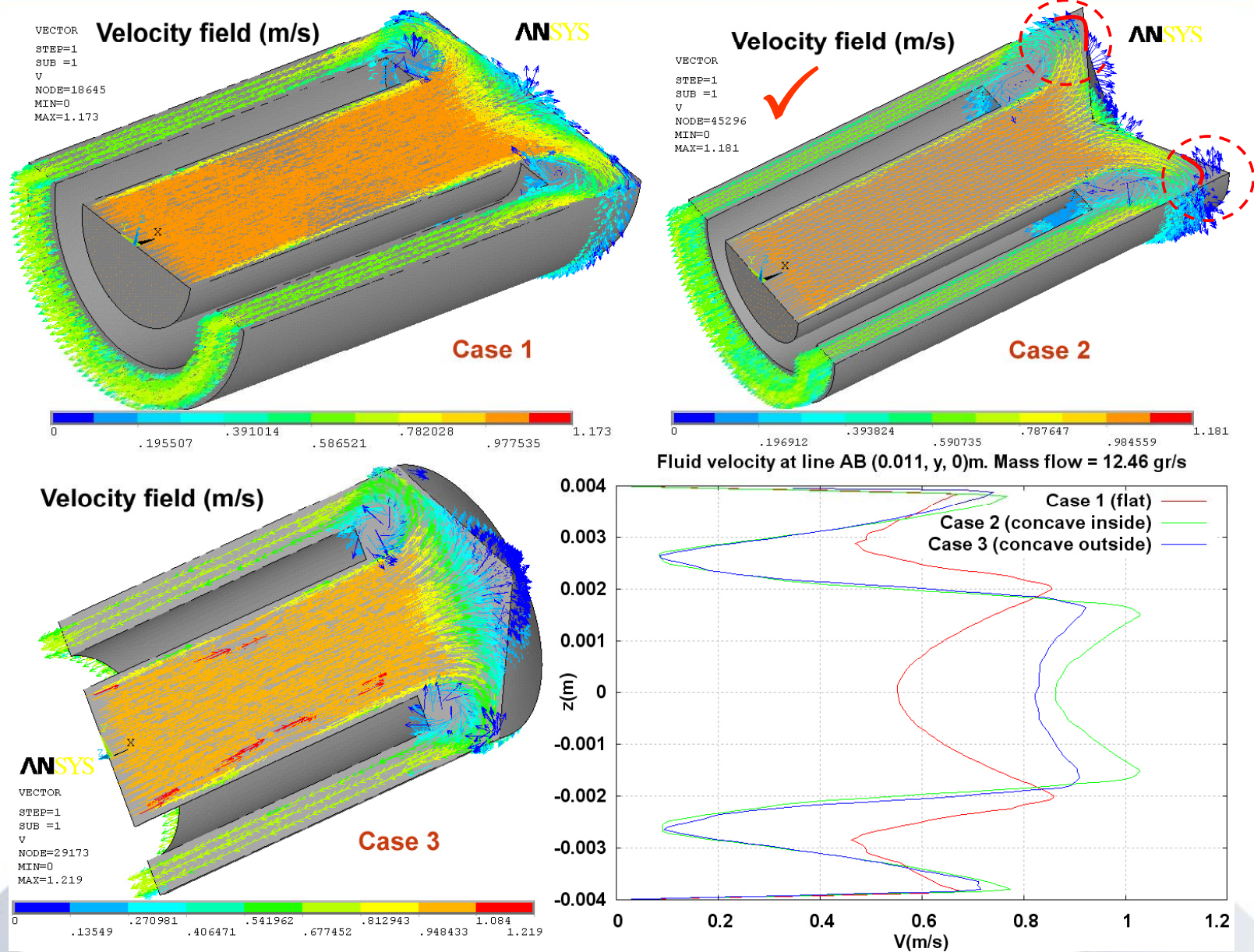


Figure 22 Velocity distributions for the three cases under investigation. The velocities curves are an example of comparative study. The results showed that the velocity field intensity for cases 2 and 3 are higher than the case 1.



Figure 23 Experimental setup for thermal hydraulic test at ALBA.

The quantification of the pressure drop is under testing, which information will be useful for the final **optimization of the hydraulic circuits** at ALBA storage ring, and obviously for the performance of the crotch absorbers.

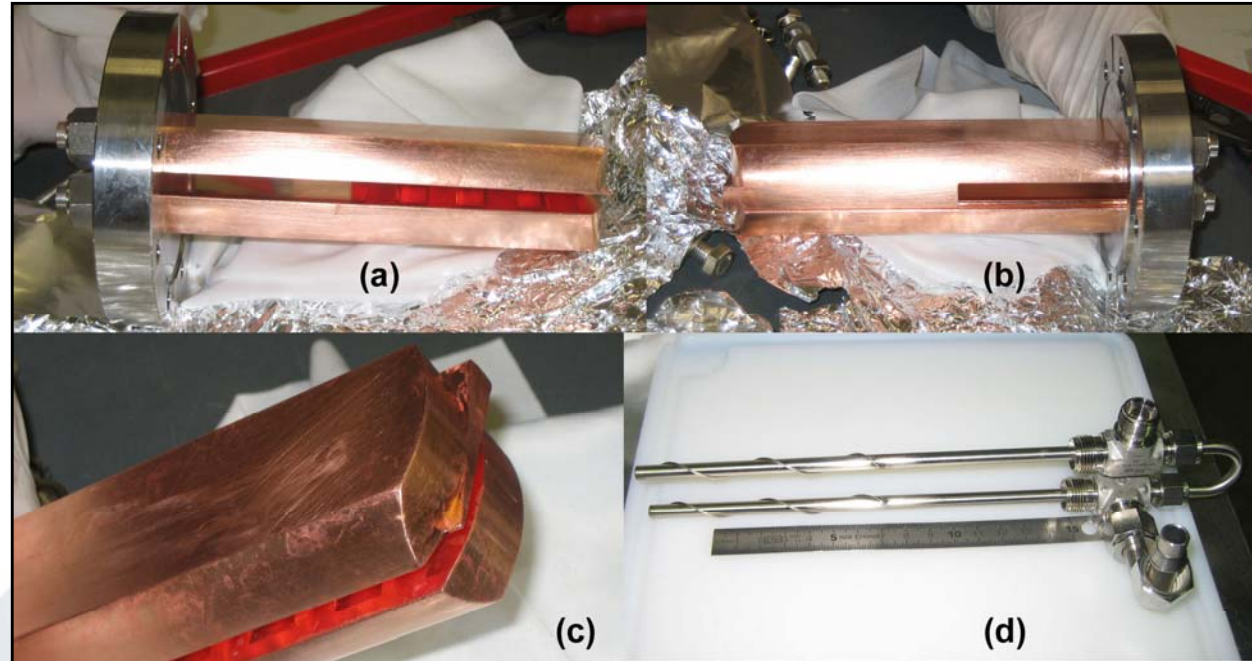


Figure 24 Pictures of a real crotch absorber at ALBA (type 1). (a) Part which receive directly the BM radiation, in between two jaws. (b) Back part of the crotch absorber. (c) Detail of the end of the crotch absorber with the “special tooth”. (d) The inner tube to be inserted into the pinholes (circular perforations at the jaws). Wires are around the inner tube in order to enhance the heat transfer.

Table 5: Verification of the pressure drop Δp at the pinholes in ALBA crotch absorbers.

<i>Flow rate = 1.7 l/min</i>			
<i>Absorber</i>	<i>Δp (bar) SLS Reference</i>	<i>Δp (bar) ALBA</i>	<i>Difference (%)</i>
<i>Type 1</i>	0.32	0.36	12.5
<i>Type 2.3</i>	0.42	0.43	2.4

1. **Design criteria**: The **cycles for fatigue** based on the **strain** are the design criteria for ALBA. The material have been chosen for values more than 1×10^5 cycles of OFHC copper (strain < 0.1%) and over 1×10^5 cycles for Glidcop (strain < 0.2%).
2. **Three types** for the crotch absorbers for ALBA.
3. The mechanical design of the absorbers has been done in a way which will guarantee the optimum performance: this include the **lowest temperature, strain and stresses** on the absorbers.
4. **An optimised design** based on **tooth thickness of 6 mm** and **inclination of 6.6°** will be used for the critical crotch absorbers. For this angle the maximum surface power density is about 28 W/mm^2
5. Based on ALBA design criteria, all the crotch absorbers are in **safe range**.